



Contents lists available at ScienceDirect

# Engineering Science and Technology, an International Journal

journal homepage: [www.elsevier.com/locate/jestch](http://www.elsevier.com/locate/jestch)



## Liquid chemical adulteration detection enhancement using a square enclosed Tri-Circle negative index metamaterial sensor

Muhammad Amir Khalil<sup>a</sup>, Wong Hin Yong<sup>a,\*</sup>, Ahasanul Hoque<sup>b,\*</sup>, Md. Shabiul Islam<sup>a</sup>, Lo Yew Chiong<sup>a</sup>, Cham Chin leei<sup>a</sup>, Saleh Albadran<sup>c</sup>, Mohamed S. Soliman<sup>d,e</sup>, Mohammad Tariqul Islam<sup>f,\*</sup>

<sup>a</sup> Faculty of Engineering (FOE), Multimedia University (MMU), 63100 Cyberjaya, Selangor, Malaysia

<sup>b</sup> Institute of Climate Change, Universiti Kebangsaan Malaysia, Bangi 43600, Malaysia

<sup>c</sup> Department of Electrical Engineering, College of Engineering, University of Hail, Hail 55211, Saudi Arabia

<sup>d</sup> Department of Electrical Engineering, College of Engineering, Taif University, P.O. Box 11099, Taif 21944, Saudi Arabia

<sup>e</sup> Department of Electrical Engineering, Faculty of Energy Engineering, Aswan University, Aswan 81528, Egypt

<sup>f</sup> Department of Electrical, Electronic and Systems Engineering, Faculty of Engineering and Built Environment, Universiti Kebangsaan Malaysia, Bangi 43600, Malaysia



### ARTICLE INFO

#### Keywords:

Metamaterial  
Oil  
Fuel  
Split Ring Resonator 'S.R.R.'  
Dielectric Constant and Loss Tangent

### ABSTRACT

This study introduces a Metamaterial 'M.M.' sensor designed and evaluated to detect pure and adulterated fuels and oils. The reflection coefficient was measured using advanced design systems and computer simulations, followed by computational and experimental analyses of the performance evolution of the proposed sensor. The proposed sensor was evaluated using samples of varying compositions of Coconut Oil 'C.O.', petrol and kerosene. The results demonstrated a noticeable change in the Resonance Frequency 'R.F.' of the samples upon modification of their concentration. The reflection coefficient values for petrol and a 20 % combination of kerosene were determined to be  $-44.81$  dB at a frequency of 10.29 GHz and  $-41.07$  dB at a frequency of 10.15 GHz. Similarly, for coconut oil and refined coconut oil, the reflection coefficient values were found to be  $-47.34$  dB at a frequency of 11.239 GHz and  $-41.981$  dB at a frequency of 11.15 GHz. The sensor exhibits a high-quality factor of 451.58, a good sensitivity value of 5.65 and a figure of merit of 2551.427, indicating its excellent performance and efficiency. The results demonstrate the versatility of the proposed sensor, making it suitable for a range of applications such as microfluidics and industrial settings.

### 1. Introduction

These days, Fuel and oil are the most ubiquitous forms of energy sources around the globe. Most fuels, including petrol, diesel, oil, and natural gas, are derived from the natural world, either dug up from the ground or manufactured through crude oil processing. There is no doubt that Fuel plays a critical role in the global economy. However, some businessmen are capitalizing on this by adding substances to the fuel supply. Particularly concerning is the rise of tainting pure Fuel with low-cost, imported Fuel in developing countries. The term 'fuel adulteration' refers to adding illegal compounds to legitimate Fuel to reduce fuel quality to a level below industry specifications. Kerosene is commonly mixed with petrol or diesel in various businesses, particularly within the

petrol station sector, with the intention of adulteration. To enhance fuel quality, certain industries and gas stations engage in the practice of blending kerosene with petrol or diesel. Adding kerosene poses the greatest risk because it drastically decreases fuel lubricity [1]. This has repercussions for a wide range of sectors, including the automotive, chemical, pharmaceutical, and food industries, among many others. Machinery using contaminated fuels suffers damage. Furthermore, if natural items involve mixing, it could have harmful effects on a wide range of organisms and ecosystems.

Consequently, scientists employed various methods in their hunt for the source of fuel adulteration. At VT MEMS Lab, [2] demonstrated the ability to identify and quantify kerosene-adulterated diesel using a partly resolved chromatogram and chemometric methods. This study

\* Corresponding authors.

E-mail addresses: [1211406090@student.mmu.edu.my](mailto:1211406090@student.mmu.edu.my) (M.A. Khalil), [hywong@mmu.edu.my](mailto:hywong@mmu.edu.my) (W.H. Yong), [ahasanul@ukm.edu.my](mailto:ahasanul@ukm.edu.my) (A. Hoque), [shabiul.islam@mmu.edu.my](mailto:shabiul.islam@mmu.edu.my) (Md.S. Islam), [yclo@mmu.edu.my](mailto:yclo@mmu.edu.my) (L.Y. Chiong), [clham@mmu.edu.my](mailto:clham@mmu.edu.my) (C.C. leei), [s.abadran@uoh.edu.sa](mailto:s.abadran@uoh.edu.sa) (S. Albadran), [soliman@tu.edu.sa](mailto:soliman@tu.edu.sa) (M.S. Soliman), [tariqul@ukm.edu.my](mailto:tariqul@ukm.edu.my) (M.T. Islam).

[3] proposes using a higher-order Bessel-Gauss beam in the context of a fiber-optic sensor to detect the amount of kerosene that has been mixed into petrol. In [4] the context of bio-sensing research, a novel Surface Plasmon Resonance 'S.P.R.' mechanism-based Photonic Crystal Fiber 'P.C.F.' biosensor has been explored to probe petrol adulteration. For evaluating the quality of diesel fuel, using the Common Dimensions Analysis 'C.D.A.', a technique performed an exploratory analysis that demonstrated that Medium-Resolution Nuclear Magnetic Resonance 'M.R.-N.M.R.' and time-domain N.M.R. are complementary methods [5]. This study [6] proposes using a higher-order Bessel-Gauss beam inside the framework of a fiber-optic sensor to determine the percentage of kerosene added to petrol. The feasibility of employing 4-Dimethylamino-Nitro-Stilbene '4-D.N.S.' molecular rotors as viscosity probes for detecting kerosene in Fuel was investigated in [7]. The present work's [8] measurement shows that ultrasonic propagation velocity can be used to detect ethanol fuel adulteration.

However, the methods mentioned above have some shortcomings in accuracy, sensitivity, efficiency, expense, and complexity in gauging the degree of adulteration [1]. Therefore, using artificial electromagnetic structures called Metamaterial 'M.M' can be extremely useful in creating straightforward and effective detectors. Metamaterials are artificial substances with unusual properties [9], such as negative refractive index ( $n < 0$ ), permittivity ( $\epsilon < 0$ ), permeability ( $\mu < 0$ ), backward wave propagation  $f(x + vt)$ , that are not typically found in natural material [10,11]. Metamaterials have attracted much interest in developing highly sensitive sensors because they display a strong electric and magnetic coupling [9]. Metamaterials can perform various applications, such as Energy Harvesting 'E.H.', perfect absorbers, cloaking and sensing mechanisms, biomedical image processing, dielectric spectroscopy and determining oil authenticity. [12–20]. It is widely acknowledged in the literature that sensors utilizing Metamaterials have demonstrated effectiveness in detecting liquid chemicals, particularly within the microwave frequency range, specifically for the 8–12 GHz. It has been demonstrated in [21] that a metamaterial-based sensor operating in the X band can be used to determine the authenticity of oil samples. The study [22] introduces a sensor that integrates fluorescence and microwave dielectric spectroscopy into a single structure, improving food quality identification. Tested on adulterated honey, it achieved good accuracy using a low-cost Visible-Near Infrared 'Vis.-NIR'. sensor, demonstrating the potential of this sensor for material characterization and identification.

The sensing study includes dielectric property measurements, such as dielectric constant ( $\kappa$ ) and loss tangent ( $\delta$ ) for chemical liquid. A metamaterial-based sensor has been proposed in [23] to detect transformer oils and other fluid materials like methanol purity and olive oil adulteration in the X-band. Experimental and simulation results show that the proposed structure's resonance frequency is affected by the dielectric constant of transformer oil or other microfluidics. Metamaterial-based sensors with oval-shaped wing resonators, transmission lines, and genetic algorithms were used to optimize the proposed structure for detecting unbranded and branded diesel in the 8–12 GHz range [24]. A microwave Metamaterial sensor built on a single Split-Ring Resonator 'S.R.R.' was proposed ref. [25] to detect the adulteration of vegetable oil and petrol blends. In ref. [26] a microwave-based portable Metamaterial-based sensor was developed to detect fuel adulteration. The dielectric characteristic has a resonance shift of 12 MHz for the fuel sample. There have been several scientific groups that have proposed various types of sensors based on Metamaterials for sensing applications, like rotation, micro-fluid, and strain[27], detection of lubricant oil [28], determination of ethanol and acetone impurities [29], determining the amount and ratio of fibers in construction materials[30], dielectric sensing in chemicals using multi-bands [31] and meta-surface sensors for biomedical applications [32]. A new method utilizing 5G millimeter-wave sensing has been developed for the detection of ethanol concentration in aqueous solutions [33]. This study [34] presents a design that utilizes metamaterials to create a dual-band

dielectric sensor for the purpose of determining the concentration of ethanol and pentane. However, the sensitivity is relatively low, and the q-factor has not been computed. This article [35] presents a microwave sensor for liquid characterization that utilizes a compact and highly sensitive mu-negative metamaterial. The primary focus of the study is on achieving miniaturization and enhancing sensitivity. To identify kerosene in oil, a Square Split Ring Resonator 'S.S.R.R.' is proposed in reference [36]. This study [37] proposes the use of a dual-band metamaterial-based sensor for determining the complex dielectric constant of ethanol-methanol mixtures. The sensitivity of this method allows for the discrimination of binary liquid mixtures at multiple frequencies due to its ability to detect resonance frequencies and its reusability. It uses the Industrial, Scientific, and Medical 'I.S.M.' band frequency of 2.47 GHz for its industrial, scientific, and medical operations, and a change in the resonance frequency of its transmission was observed. A fuel authenticity sensor based on an omega-shaped resonator can detect imposter samples of fuels such as petrol, engine oil, diesel, waste, and clean transformer oil by analyzing their dielectric properties [38]. To distinguish between branded and unbranded oils and fuels samples in frequency region 8–12 GHz, an oval-shaped wing resonator-based sensor inspired by Metamaterials is designed and fabricated. The experimental and simulation outcomes indicate that the proposed structure is more sensitive than previously reported, but there is no calculation of the Quality Factor 'Q-Factor'. The previous research exhibits limitations, such as the low or uncalculated q-factor and sensitivity. To effectively tackle these concerns, this study aimed to enhance sensing capabilities while simultaneously improving sensing resolution to address these concerns effectively.

The objective of this study is to enhance the detection of fuel adulteration through the utilization of a small-scale sensor based on Metamaterials. This design consists of a square enclosure that contains three compact split-ring resonators. A number of expensive and complex methods were presented in the literature for detecting fuel adulteration, which prompted the present study. The present study was motivated by the existence of costly and intricate techniques described in the literature for identifying fuel adulteration. The new enhancement of this study lies in the integration of small tri resonators enclosed within a square structure, which forms a unified sensor framework. This integration allows for the effective detection of contaminated Fuel. Furthermore, the sensor possesses the capability to quantify dielectric characteristics. The proposed low-cost sensor exhibits favourable quality factors, sensitivity, and resolution features, making it suitable for real-time applications, specifically for verifying the authenticity of liquid chemicals at X-band frequencies.

## 2. Material and design methodology

**Fig. 1 (a)** illustrates a schematic illustration of the sensor that has been proposed. The design configuration consists of split-ring resonators, where tri-circular split-ring resonators enclosed in a square are applied onto the substrate's front and back sides, creating a distinctive metamaterial sensor. The numerical analysis and optimization of the sensor geometry were conducted using the full-wave Finite Integration Technique 'F.I.T.', based on the high-frequency electromagnetic solver in Computer Simulation Technology 'C.S.T.' 2022. Three primary layers constitute the sensor under consideration: the resonator, sensor layer, and dielectric substrate. The resonator is constructed from copper metal, which has a thickness, thermal conductivity and electric conductivity of 0.035 mm, 401 W/Km and  $5.8 \times 10^7 S/m$  respectively. On the posterior side of the Square Enclosed Tri Circular Split Ring Resonator 'S.T.C.S.R.R.' resonator, a sensor layer of  $10 \times 10 \times 10 mm^3$  in length was precisely positioned, as depicted in **Fig. 1(b)**. The dielectric substrate utilized in this study is composed of FR-4 with a thickness of 1.524mm. It exhibits a relative permittivity of 4.30 and a loss tangent of 0.02. This study selected FR-4 as a substrate based on its advantageous characteristics,

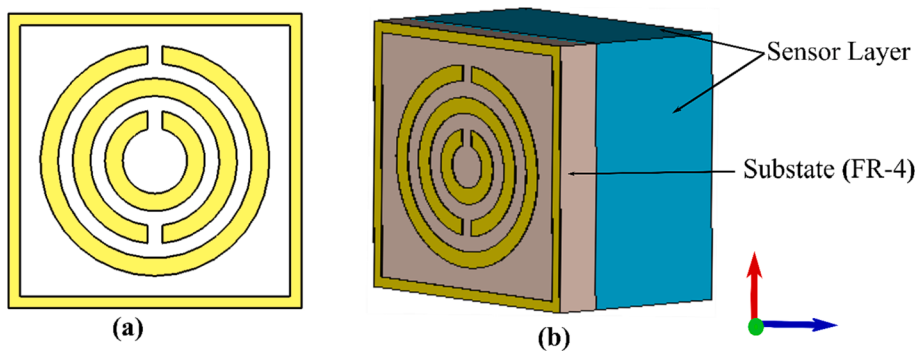


**Fig. 1.** The proposed M.M sensor based on T.C.S.R.R (a) Front view (b) Perspective view.

including low loss, affordability, and mechanical strength.

The unit cell of the proposed structure is depicted in Fig. 2, with dimensions of 10mm in length, 10mm in width, and 1.524mm in height. The additional significant aspects of the sensor under consideration, as depicted in Fig. 2(a) and 2(b), were chosen through a combination of our prior research findings and the application of the C.S.T. optimization technique. An illustration of the overall dimensions of our proposed metamaterial sensor is shown in Fig. 2 (a). In order to streamline the simulation procedures and facilitate the dimensional optimization of the suggested Metamaterial sensor, different boundary conditions, such as Perfect Electrical and Magnetic Conductors 'P.E./P.M.C.', free space, and pattern distribution, were implemented through microwave analysis techniques. The implementation of the Perfect Electrical Conductor 'P.E.C.' boundary condition was incorporated in both the x- and y-directions within this design, as depicted in Fig. 2(b). The aforementioned boundary condition is predicated on the assumption that the conductor in question is an ideal conductor possessing negligible electrical resistance, thereby facilitating the complete reflection of incident electromagnetic waves. On the other hand, the z-axis was designated as an open boundary. This means there is no constraint or reflection in the z-direction, allowing the electromagnetic waves to propagate freely in that direction.

### 3. Different parametric study

Fig. 3 illustrates a detailed configuration of the proposed architectural design for the sensor, showcasing each step in a sequential manner. The first design demonstrates that the reflection coefficient ( $S_{11}$ ) value is  $-0.073$  dB at 11.292 GHz by placing a square shape on the substrate. When a square shape and a single ring are placed on the substrate (FR-4), the  $S_{11}$  value is  $-8.625$  dB at 11.14 GHz. In the third design,

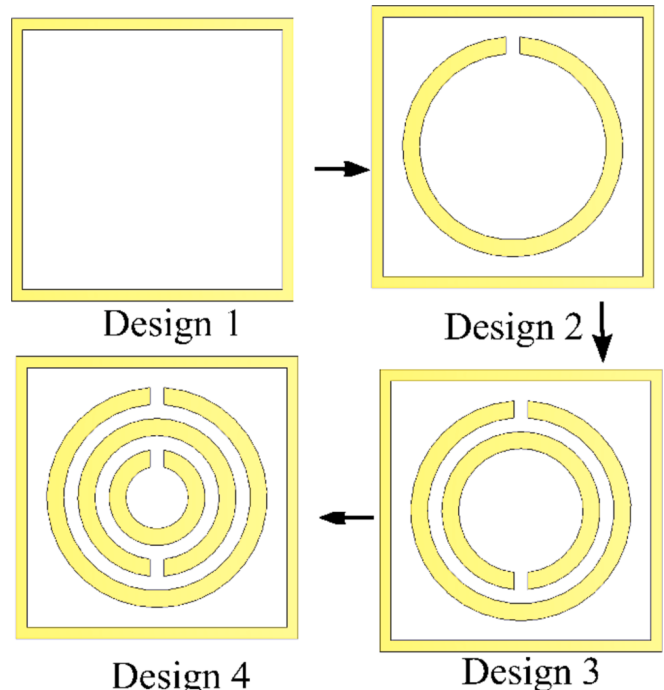


**Fig. 3.** Step-by-Step design evolution

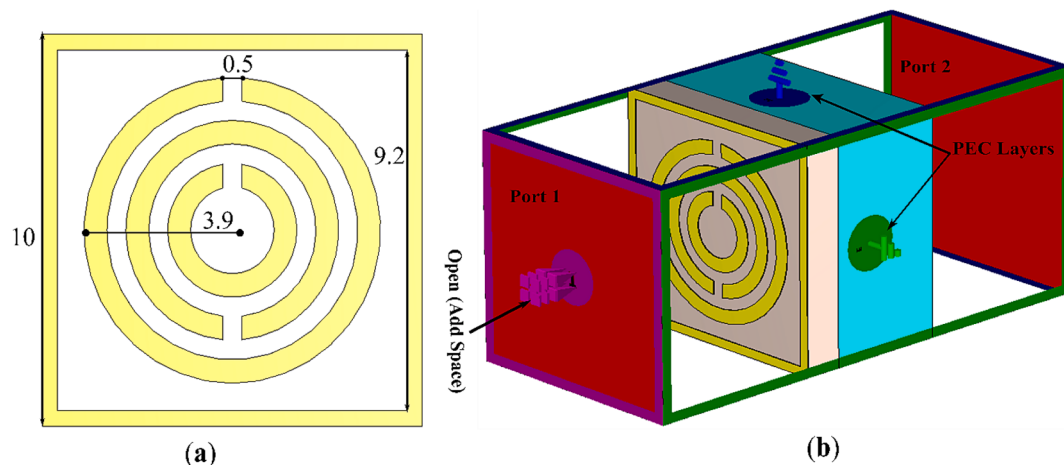


**Fig. 2.** (a) Perspective view with dimensions (b) Simulation setup for the proposed M.T.M.

simulation results indicate  $S_{11}$  value of  $-8.62$  dB at  $11.168$  GHz by arranging a square shape and two rings on the substrate. In the fourth and final design simulation,  $S_{11}$  value of  $-47.09$  dB is displayed at a frequency of  $11.292$  GHz. This objective can be achieved by arranging a square structure and three circular formations on the substrate. The values of the reflection coefficients for the various stages of the recommended M.M. sensor are shown in Fig. 4. As a result, the final sensor developed is a metamaterial based on a square-enclosed tri-ring splitting resonator.

Fig. 5 illustrates the impact of a number of different split gap values on the resonance frequency. A significant effect on resonance frequency can be observed when the split gap variation ranges between  $0.5\text{mm}$  and  $1.0\text{mm}$ , with increments of  $0.2\text{mm}$  and  $0.3\text{mm}$ . Based on Eq. (1) [35], we can derive a relationship between the resonance frequency and split gap.

$$f = \frac{1}{2\pi\sqrt{LC}} \quad (1)$$

In light of the above equation, frequency and capacitance are inversely proportional. Table 1 demonstrates an inverse relationship between frequency and split gap.

In order to determine which substrate material is the most suitable for the design that has been suggested, as well as to assess the performance of each of the substrate materials, three distinct substrate materials were evaluated. A comparative analysis has been conducted on the physical characteristics of three substrates, namely FR-4, Rogers RO-4350B, and RT-3010. A FR-4 substrate is characterized by a thickness of  $1.524\text{ mm}$ , dielectric constant ( $\kappa$ ) and loss tangent ( $\delta$ ) are  $4.3$  and  $0.0250$ . In the case of the RO-4350B substrate, it has a thickness of  $1.524\text{ mm}$ , dielectric constant ( $\kappa$ ) and loss tangent ( $\delta$ ) are  $4.6$  and  $0.037$ . In addition to the thickness of RO-3010B,  $1.27$ , the dielectric constant ( $\kappa$ )  $10.20$  and loss tangent ( $\delta$ )  $0.00220$ , respectively.

$$C = \epsilon_0 \epsilon_r \frac{A}{d} \quad (2)$$

As per Eq. (2) proposed by reference [39,40], the concept of equivalent or total capacitance is elucidated. The symbol  $\epsilon_0$  represents the permittivity of free space, which is equal to  $8.854 \times 10^{-12}\text{F/m}$ . The variable  $\epsilon_r$  and  $d$  represented relative permittivity and split gap and area.

According to Eq. (2), variable C exhibits a direct proportionality with the permittivity. Hence, it is evident that different substrates display unique permittivity values, resulting in discrepancies in resonance

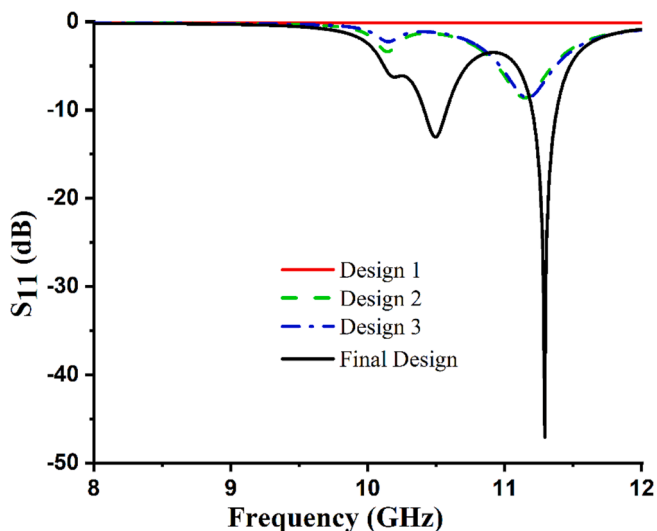


Fig. 4. Reflection coefficients ( $S_{11}$ ) for the various stages of the recommended M.M. sensor.

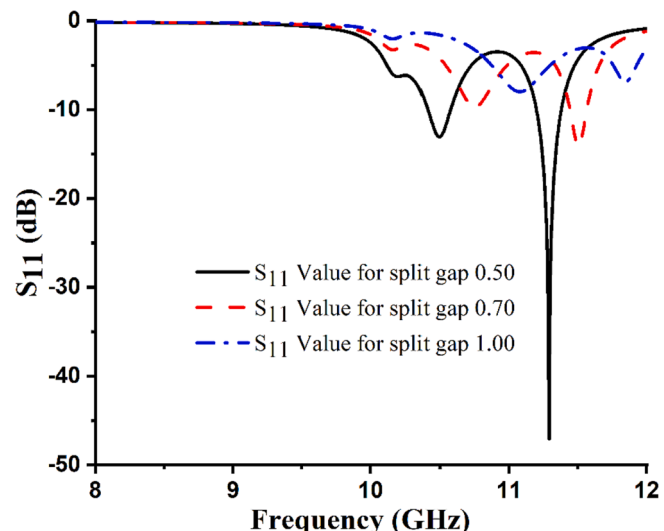


Fig. 5. Influence of various Split gaps on the R.F.

**Table 1**  
Relationship between the R.F. and the split gap.

S.No.	Split Gap	Frequency (GHz)	Reflection Coefficient Value(dB)
1	0.50	11.292	-47.07
2	0.70	11.516	-14.50
3	1.00	11.86	-6.93

frequency. Consequently, the resonance frequency of the unit cell exhibits an upward shift when the substrate permittivity decreases and, conversely, a downward shift when the substrate permittivity increases. The graphical representation in Fig. 6 illustrates the correlation between the frequency and reflection coefficient values across various substrate materials.

The determination of the equivalent inductance is derived from Eq. (3) [41], based on the fundamental principle of the transmission line.

$$L(nH) = 2 \times 10^{-4} l \left[ \ln \left( \frac{l}{w+l} \right) + 1.193 + 0.02235 \left( \frac{w+t}{l} \right) \right] K_g \quad (3)$$

Eq. (3) defines the variables  $l$ ,  $w$ ,  $t$ , and  $K_g$ , which respectively represent the length, width, and thickness of a microstrip line. The variable  $K_g$  represents the correction factor.

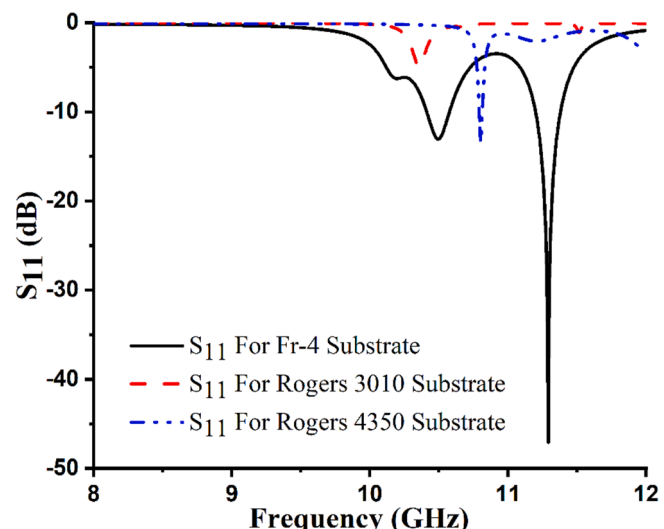
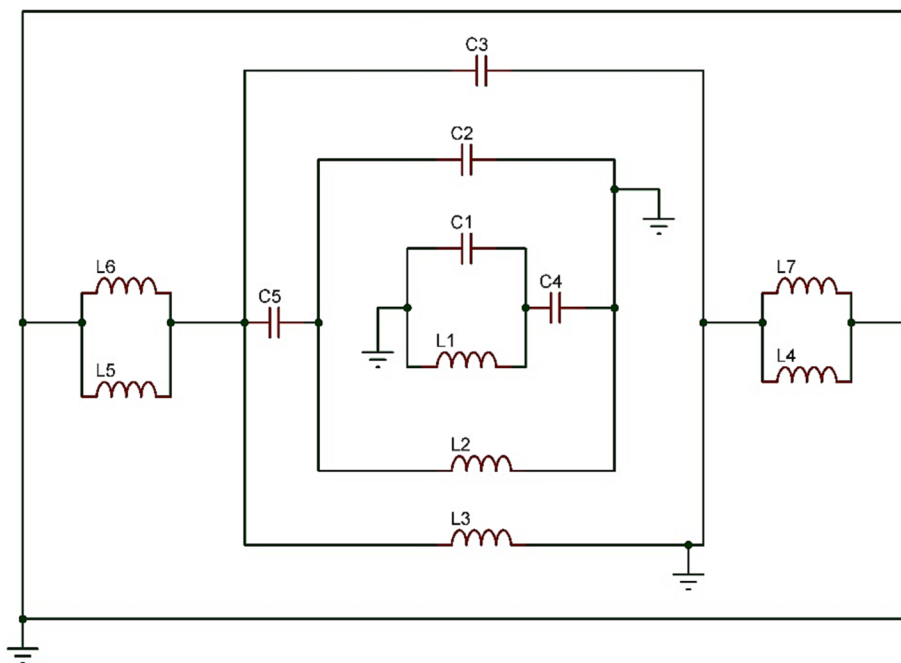


Fig. 6. Frequency vs Reflection Coefficient for different substrate.



**Fig. 7.** Equivalent Circuit Diagram In A.D.S.

**Fig. 8** illustrates the reflection coefficient acquired from the C.S.T. and Advance Design System 'A.D.S.' and **Fig. 7** circuitry diagram. Several factors could explain the discrepancies observed between C.S.T. and A.D.S. reflection coefficients. It can be argued that all of the C.S.T. simulation setup's parameters are stable; one could argue that the simulation reflection coefficient of the C.S.T. is also stable [9]. In an alternative approach, A.D.S. results can be acquired by manipulating the capacitor and inductor values within the equivalent circuit. The reason for this is the slight disparity in value between capacitors and inductors. The values for capacitors and inductors are provided in **Table 2**.

To better understand the underlying mechanism of the sensor's design, surface current and electric field distribution were analyzed. By analyzing the surface current and electric field distribution, we can gain insight into the energy contained within the device and the associated losses. The generation of an electric field occurs within the space between the capacitive plate of the Complementary Split-Ring Resonator 'C.S.R.R.' and the enclosed resonator during resonance. Consequently, the area immediately surrounding and within the C.S.R.R. becomes sensitive to changes in the dielectric properties of the material. Consequently, the region containing the C.S.R.R. is suitable for evaluating the dielectric properties of various materials. There is a greater concentration of electric field strength in the components of the resonator, particularly in the capacitive elements of the resonator, as illustrated in **Fig. 9 (a)**. **Fig. 9 (b)** illustrates the simulation distribution of surface currents at the resonance frequency of 11.292. Furthermore, it should be noted that more currents circulate within the left and right sides of the resonator, controlling the electromagnetic and electric signals, respectively. The simulated distribution of surface currents for the suggested

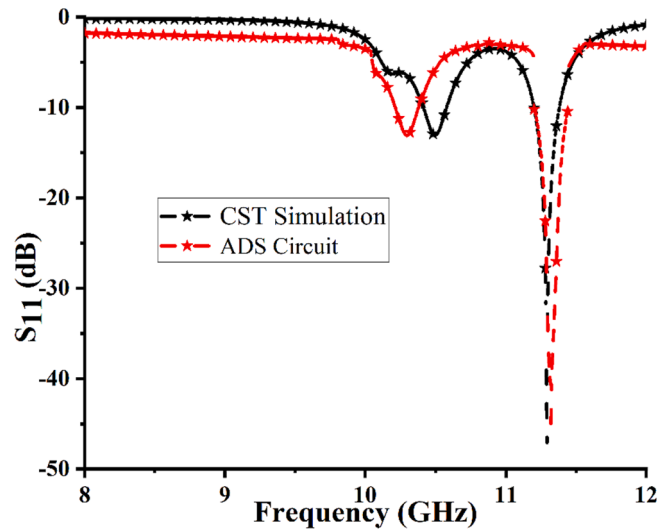


**Fig. 8.** Simulated S<sub>11</sub> in C.S.T. and A.D.S.

structure serves as a definitive indication of the existence of the electric dipole responsible for generating the resonance phenomena.

#### 4. Simulated and measured sensor analysis

This study aimed to examine the sensor's potential in detecting different types of oil samples. The placement of the resonators occurs on both sides of the substrate. A reservoir thickness of 10mm was designated for the sensor layer to accommodate different types of oils. In this configuration, the magnetic field of the transmitted electromagnetic wave is oriented perpendicular to the sensor layer along the z-axis. The waveguide's ports 1 & 2 were affixed to both sides of the designated structure's surfaces to conduct numerical analysis and experimental testing of the reflection response, specifically S<sub>11</sub>. The C.S.T. simulation was utilized to obtain the real and imaginary components of the relative permeability ( $\mu$ ), relative permittivity ( $\epsilon$ ) and refractive index (n) of the

**Table 2**  
Inductor and Capacitor Value for Equivalent Circuit.

Inductor	Value (nH)	Capacitor	Value(pF)
L1	0.00147	C1	10.006
L2	0.0044	C2	17.80
L3	200.003	C3	46.204
L4	109.974	C4	0.058
L5	4.573	C5	70.014
L6	0.605		
L7	1.05		

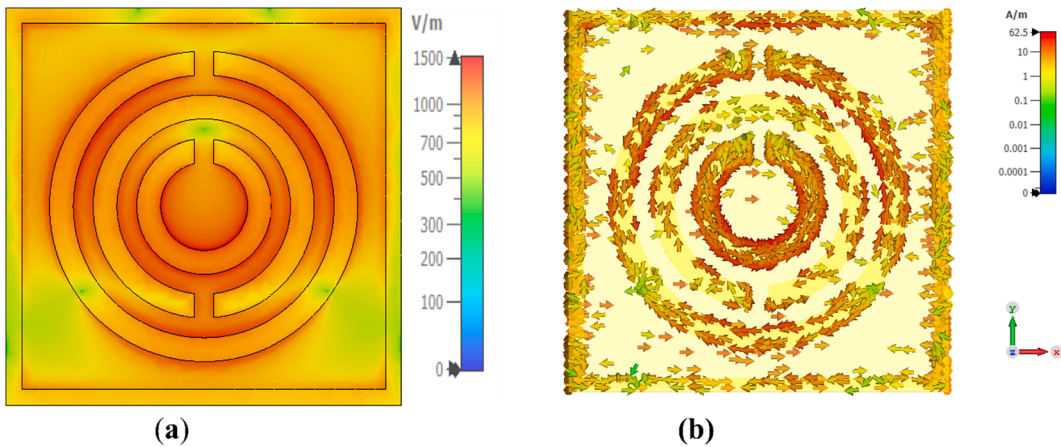


Fig. 9. Electric field (a) Surface Current Distribution (b) at 11.292 GHz.

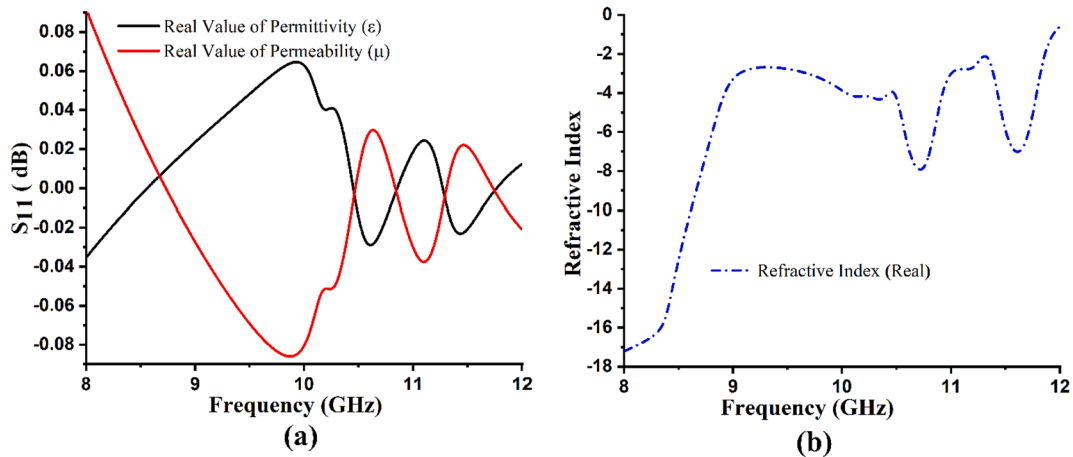


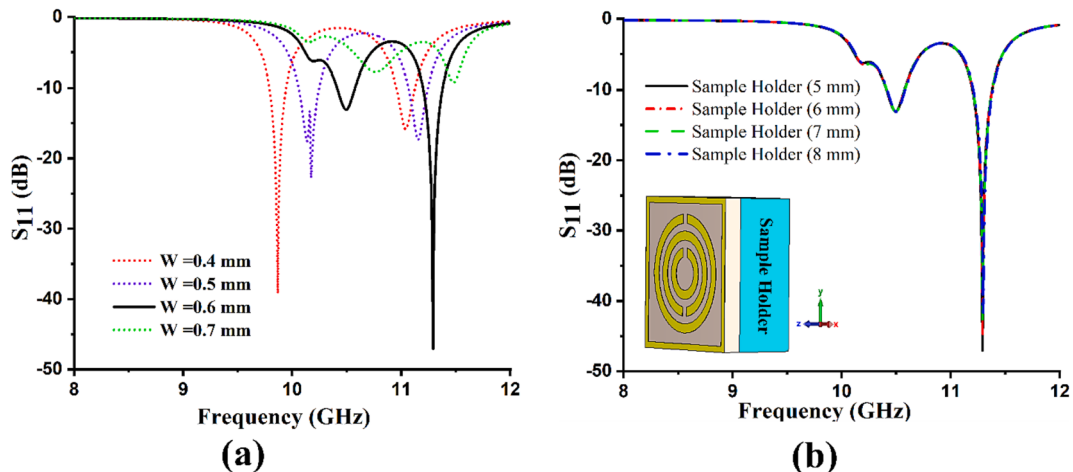
Fig. 10. Effective parameters: (a) permeability and permittivity; and (b) refractive index (n).

**Table 3**  
Double negative value at various resonance frequencies.

S.No.	Frequency (GHz)	D.N.G. Value
1	10.464	-0.0049
2	10.484	-0.0037
3	11.292	-0.00427

sensor. These properties are depicted in below Fig. 10 (a,b) for the purpose of unveiling the metamaterial characteristic. The Double Negative 'D.N.G.' value for the suggested sensor is depicted in Table 3. This observation suggests that the resonator structure under consideration exhibits potential M.M. properties.

$$L = \frac{d}{2\pi\mu f A} \quad (4)$$

Fig. 11. Impact of Resonator Width and Sample Holder Size on Reflection Coefficient (S<sub>11</sub>).

Eq. (4) is obtained through the derivation process involving Eqs. (1) and (2). According to Eq. (4), it can be observed that the width of the resonator exhibits an inverse relationship with the inductance. Additionally, the inductance demonstrates an inverse relationship with the Resonant Frequency ' $f_0$ '. Consequently, an increase in the width of the resonator leads to an increase in  $f_0$ . The  $f_0$  of the sensor under consideration has been affected by the width of the resonator, as depicted in Fig. 11 (a). The simulation was conducted under the condition of an empty sample holder to illustrate the observed shifts in resonance frequency. We observed the effect of changing the resonance frequency on the proposed sensor by altering the resonator width. The resonator utilized in this sensor based on the M.M. technique exhibits four distinct widths, which are 0.4, 0.5, 0.6, and 0.7 mm.

The modification of the sample holder also affects the resonance frequency. The dimensions of the sample holder were augmented by 1 mm, commencing at 5 mm and concluding at 8 mm. Fig. 11 (b) depicted the graphical representation of the simulation's impact on the sample holder due to adulteration.

The dielectric properties of different oils and fuels were measured using the experimental setup depicted in Fig. 12. The dielectric properties of each sample, including the dielectric constant and loss tangent, were analyzed using a coaxial probe kit and a Power Network Analyzer 'P.N.A.-L N5224'. The samples analyzed included Coconut Oil, petrol and a mixture of petrol with a 20 % kerosene ratio. A crucial step in this measurement involves the calibration of the Vector Network Analyzer 'V.N.A.' within the microwave frequency specified range of 8 to 12 GHz. The experiments were conducted at 25 degrees Celsius, generally accepted as the standard room temperature. Before conducting measurements on the selected samples, the apparatus was calibrated. To initiate the calibration procedure, the V.N.A. was equipped with the dielectric property data of pure water. The dielectric component was kept inactive during this process, and measurements were taken for air. A measurement was performed to assess the dielectric characteristics of water with the purpose of achieving accurate calibration of the V.N.A. Subsequently, an assessment was carried out to measure the dielectric properties of the chosen samples.

In order to validate the outcomes of the simulation, a sensor was constructed by fabricating a square structure that encloses triple-circle split-ring resonators. This fabrication process was carried out using the Leiterplatten-Kopierfrasen' L.P.K.F.' ProtoMat S103 circuit board plotter. This particular plotter is commonly utilized for the production of prototypes of printed circuit boards 'P.C.B.'. The illustrated diagram in Fig. 12 highlights the fabricated design of the proposed structure. The

resonator was constructed using copper material placed on both sides of substrate surfaces. The experimental investigations were conducted using the Agilent PNA-L series N5227A V.N.A., coaxial cable, two waveguide ports, one extended port, and a sample holder. The frequency range utilized in the experiment was set from 8 to 12 GHz (GHz).

The experimental configuration consisted of employing a sample holder made from an acrylic sheet with a depth of 10 mm. In oil insertion, the sample holder is furnished with an upper gap-sealed using an identical material to alleviate any potential adverse effects on the surrounding environment. In order to mitigate the risk of the potential for cross-contamination between the cooking oils and fuel samples, a separate sample holder was assigned to each oil sample. A syringe was employed for the purpose of introducing a precise quantity of oil sample into the sample holder. During experimental work, it is necessary that all experimental work be done at room temperature. Temperature fluctuations can cause alterations in the electrical and magnetic characteristics of these materials. In order to ensure the validity of the results, the suggested sensor sample holder was filled with a mixture of petrol and kerosene, with a 20 % kerosene content.

The sample holder has a volume of 1000 mm cube. It is filled with liquid samples at various capacities, including 10 %, 20 %, 40 %, 60 %, 80 %, and 100 %. It is not possible to obtain accurate and reliable results when the sample holder is only filled to 10 % of its volume. We can achieve more precise and reliable outcomes when the volume of liquid in the sample holder is 20 % or higher. The comprehensive experimental procedure for quantifying the reflection coefficient of various oil samples is illustrated in Fig. 13.

## 5. Coconut oil and refined coconut oil analysis

The quality of different types of oil can exhibit variation due to the composition of their constituent elements and the prevailing environmental conditions. Hence, it was anticipated that the dielectric properties of the oil could be employed as a viable approach for assessing quality assurance and appraising the health benefits it provides. The extraction of Coconut Oil 'C.O.' involves obtaining it from the matured coconuts harvested from the coconut palm. This oil is characterized by its high content of saturated fats. C.O. is obtained through a refining process involving high temperatures (204–245 degreesC) [42], which facilitates the extraction of its substantial saturated fat content. As a result of the refining process, C.O. does not have taste and fragrance. In contrast, Virgin Coconut Oil 'V.C.O.' is obtained from the mature and fresh kernels of coconuts using mechanical methods, with or without the

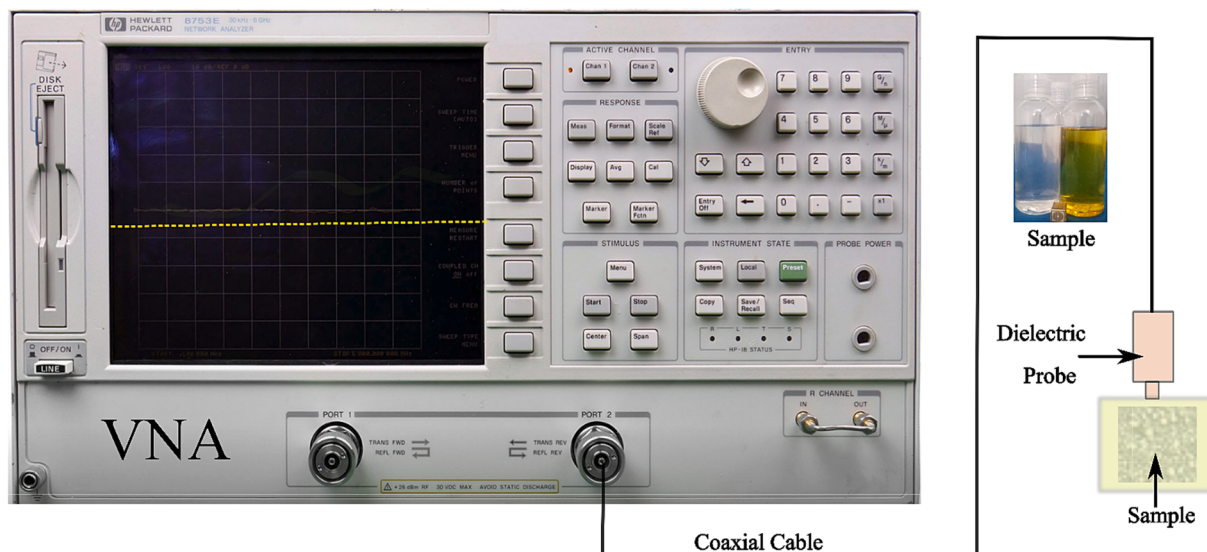
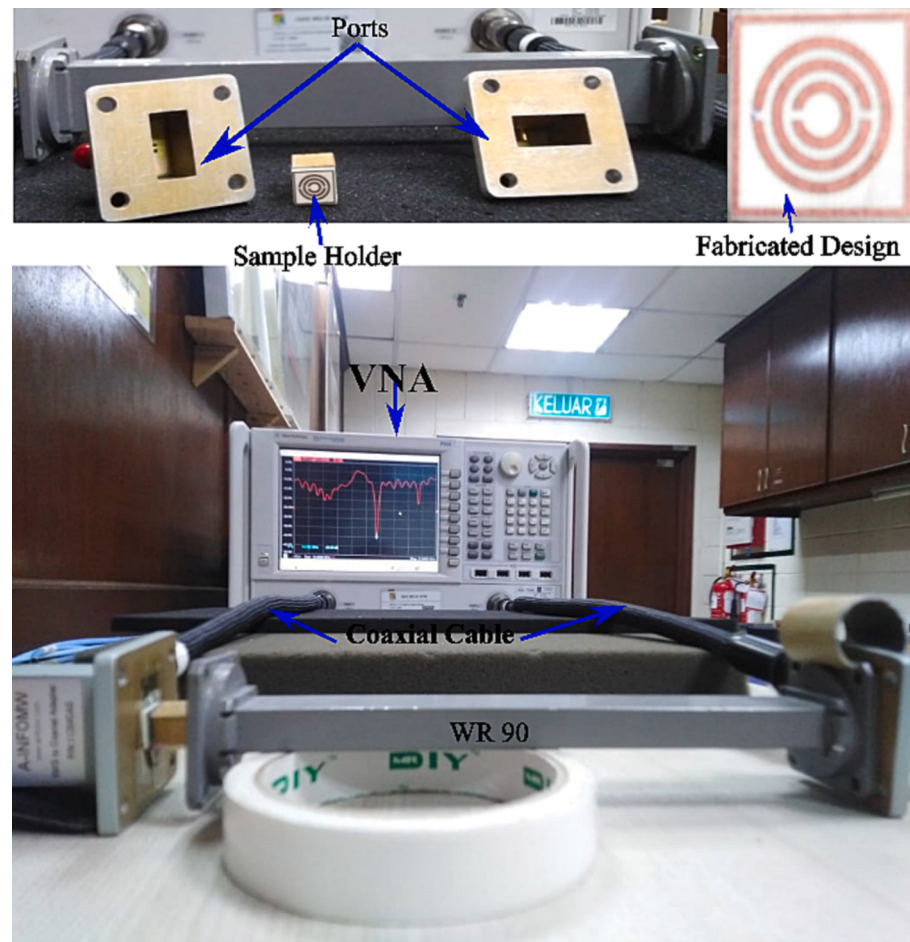


Fig. 12. The experimental setup for measuring the dielectric properties of samples.



**Fig. 13.** Experimental step for measurement  $S_{11}$  for different samples, fabricated design, sample holder and ports.

use of heat, and without undergoing any chemical refining procedures. In acquiring V.C.O., preserving its taste and fragrance is accomplished by refraining from employing chemical treatment and heating procedures [42].

The dielectric constant and loss of tangent of C.O. and V.C.O. were determined using a dielectric measurement kit within the frequency range of 8 to 12 GHz, as illustrated in Fig. 14(a,b). Fig. 14(a) depicts the dielectric constant of the C.O. and V.C.O. oil samples. The plots show that the dielectric constant of C.O. and V.C.O. is approximately 2.15 and 2.27, respectively, at a frequency of 8 to 12 GHz. Fig. 14(b) depicts the

Loss of Tangent values of the C.O. and V.C.O. samples. The plots illustrated the dielectric constants of C.O. and V.C.O. at a frequency of 8 GHz, with approximate values of 0.278 and 0.22, respectively.

Based on simulation and measurement data, the reflection coefficient ( $S_{11}$ ) outcomes for C.O. and V.C.O. are showcased in the X-band frequency range, as illustrated in Fig. 15 (a,b). Fig. 15(a,b) depict three graphical representations, namely the empty sample holder, the simulated oil value, and the experimental oil value obtained after the injection of the oil sample into the sample holder.

The simulation value of the reflection coefficient ( $S_{11}$ ) with an empty

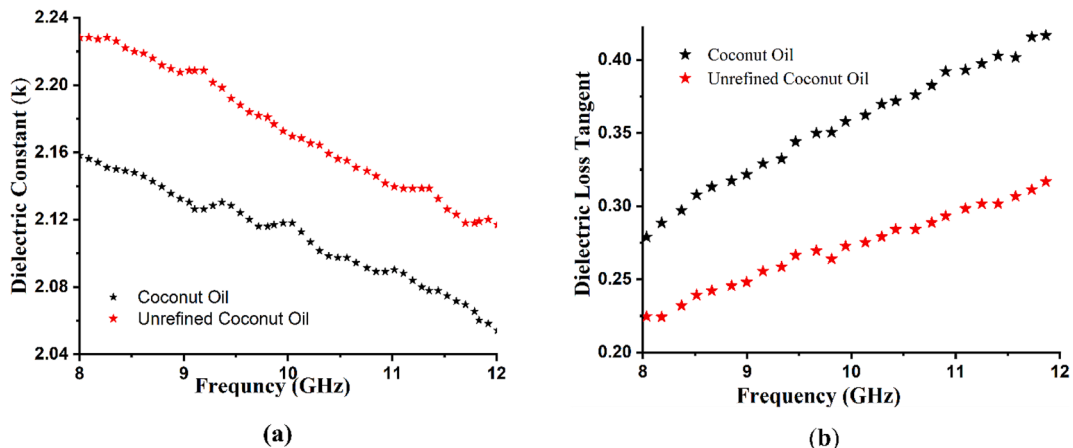


**Fig. 14.** The measured values for samples of coconut oil and Virgin coconut oil: (a) Dielectric Constant (b) Loss of Tangent.

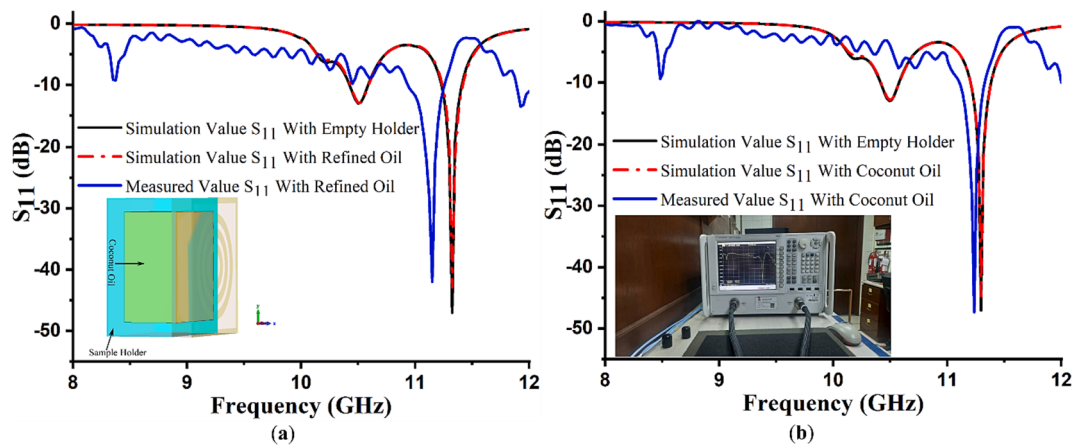


**Fig. 15.** Simulation and measurement value of  $S_{11}$  (a) Refined Coconut Oil (b) Virgin Coconut Oil.

sample holder is  $-47.07$  dB at a frequency of  $11.292$  GHz. When we put a sample of oil during the simulation process, the simulated value of the reflection coefficient ( $S_{11}$ ) for coconut oil was  $-44.897$  dB at a frequency of  $11.292$  GHz and measured  $-47.34$  dB at a frequency of  $11.289$  GHz for V.C.O., as depicted in Fig. 15 (b). In addition, the recorded value of  $S_{11}$  magnitude for C.O. is  $-44.34$  dB at a frequency of  $11.239$  GHz, while the measured value for refined coconut oil is  $-41.981$  dB at  $11.15$  GHz, as depicted in Fig. 15 (a). The results demonstrate that the simulated and experimental results exhibit high similarity, indicating that the proposed design has been accurately fabricated and effectively tested. It is important to note that the proposed structure can effectively differentiate between the various liquid samples positioned within the sample holder.

## 6. Pure petrol and refined petrol (Kerosene) analysis

Fuel adulteration and sensing application are critical to ensuring fuel quality. During the study's second phase, an investigation was conducted to assess fuel adulteration, which holds significant importance in discerning the good quality of petrol compared to kerosene. The computational and experimental studies were carried out using a sensor layer filled with petrol and kerosene in the proposed structure. The electromagnetic properties of petrol and a mixture containing 20 % kerosene in petrol, specifically the dielectric constant and dielectric loss factor, were determined using the N1500A kit as illustrated in Fig. 16 (a, b). Fig. 16 (a) depicts the dielectric constant of petrol and a mixture containing 20 % kerosene samples. The plots illustrate that the dielectric constant of petrol and a mixture containing 20 % kerosene is

approximately 2.57 and 2.37, respectively, at a frequency of 8 GHz. Fig. 16 (b) depicts petrol's Loss of Tangent values and a mixture containing 20 % kerosene samples. The plots illustrated the dielectric constants of petrol and a mixture containing 20 % kerosene at a frequency of 8 GHz, with approximate values of 0.134 and 0.143, respectively.

The collected data has been utilized as input for simulation purposes using C.S.T. Microwave Studio to verify the obtained results through both simulation and experimental approaches. Fig. 17 (b) depicts the pure petrol sample's simulated and measured reflection coefficient plot. Based on the graph, it is evident that the simulated value for pure petrol is  $-44.88$  dB at a frequency of  $10.29$  GHz, whereas the measured value is  $-44.81$  dB at a frequency of  $10.29$  GHz. When petrol is mixed with a volume proportion of 20 % kerosene, the resonance frequency of the reflection coefficient moves from  $11.292$  GHz to  $10.15$  GHz, and the signal level ( $S_{11}$ ) drops from  $-44.209$  dB to  $-41.07$  dB, as depicted in Fig. 17(a).

The measured results and simulated outcomes are in concurrence. Discrepancies between simulated and measured data may arise due to the mutual coupling effect of the waveguide port, manufacturing tolerances, and measurement error. Furthermore, the mutual resonance between the transmitting and receiving terminals of two waveguide ports will invariably influence the measurements, which leads to a slight discrepancy in both data sets.

## 7. Analysis of quality factor, sensitivity, and figure of merit (FoM)

When exploring dielectric properties, the quality factor is a crucial

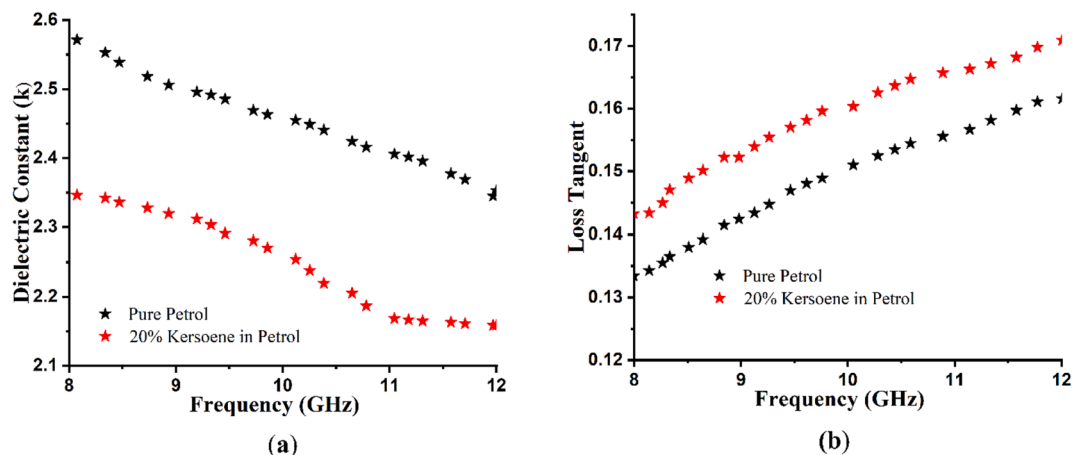


**Fig. 16.** The measured values for samples of pure petrol and 20% kerosene in petrol: (a) Dielectric Constant (b) Loss of Tangent.

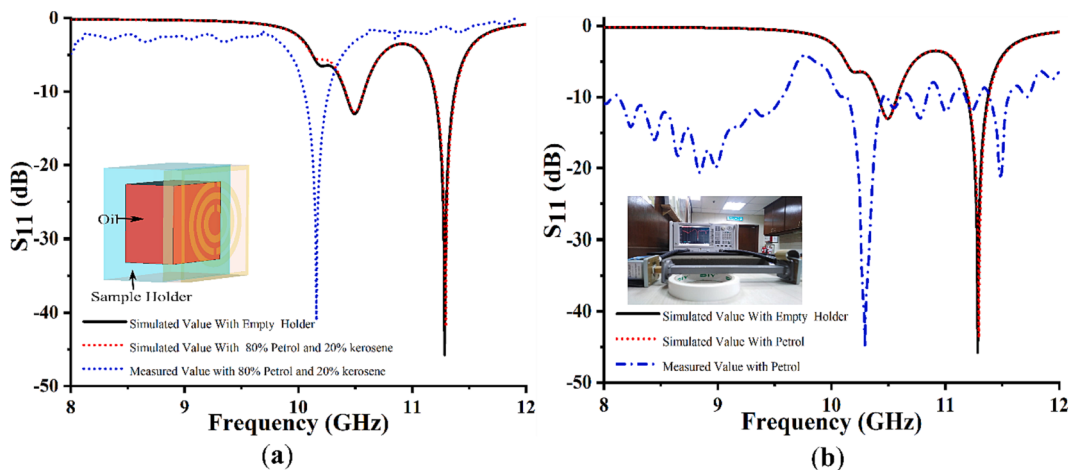


**Fig. 17.** Simulation and measurement value of S11 (a) 80% Petrol and 20% kerosene Oil (b) 100% Petrol.

consideration in the context of Metamaterial-based sensors. In the preceding study, most papers on sensing applications utilizing Metamaterials exhibited low-quality factors or lacked experimental measurements. The Q-factor is determined by the ratio of the centre frequency (the resonant frequency) to the bandwidth. The quality factor for the proposed sensor can be determined by utilizing the Eq. (5) referenced in [9].

$$Q.F. = \frac{f_r}{\Delta f} \quad (5)$$

In the given equation, the symbol “f” represents the resonance frequency, while “delta f” represents the combined values of the higher and lower cutoff frequencies. Based on the M.M. principle, the sensor under consideration demonstrates a q-factor value of 451.58.

Eq. (6) below represents the calculated sensitivity [43], denoted as S, which is expressed as a percentage

$$S(\%) = \frac{f_o - f}{f(\epsilon_r - 1)} \quad (6)$$

The variable  $f_o$ ,  $f$  and  $\epsilon_r$  denote the resonance frequency in the absence of a sample in the holder, the resonance frequency in the presence of a sample in the holder, and the permittivity of the sample, respectively. The sensitivity value for the proposed sensor is 5.65. The Figure of Merit (FoM) is determined by the equation  $FoM = S \times Q$ , as referenced [9].

Table 4 presents a comparative analysis of the M.M.-inspired sensor, as presented in the study, and other sensors discussed in the research. Several factors are compared in this study, including the size of the sensor, the substrate materials used, the frequency range of operation, the frequency shift seen, the quality factor of the sensor, and the various applications in which it can be utilized. The comparative analysis

presented in Table 4 demonstrates that our suggested work outperforms alternative solutions in terms of performance. The sensor exhibits a quality factor of 451.58, indicating its ability to maintain high performance and efficiency. Additionally, it demonstrates a high sensitivity of 5.65, further highlighting its effectiveness in detecting and measuring signals. The figure of merit, quantified at 2551.427, further reinforces the sensor's overall excellence in terms of its performance and efficiency.

## 8. Conclusion

In this study, the design and fabrication of a metamaterial sensor was successfully employed for detecting adulterated fuels and oils within the frequency range of 8 to 12 GHz. The efficacy of the structure, with regard to its performance, has been substantiated through comprehensive analysis encompassing both theoretical and empirical examination. The dimensions of the designed structure are  $5 \times 5\text{mm}^2$ . The surface current and electric field distribution analysis has been conducted, and an analogous circuit analysis has been performed to validate the chosen design. The simulated reflection coefficient values for pure petrol and a 20 % mixture of kerosene in petrol are  $-44.88$  dB and  $-44.209$  dB, respectively. Similarly, the reflection coefficient values for coconut and refined coconut oil are  $-44.897$  dB and  $-44.34$  dB, respectively. The measured reflection coefficient values were found to be  $-44.81$  dB at a frequency of 10.29 GHz,  $-41.07$  dB at a frequency of 10.15 GHz,  $-47.34$  dB at a frequency of 11.239 GHz, and  $-41.981$  dB at a frequency of 11.15 GHz. The study's findings suggest that the proposed sensor outperforms previously reported sensors in terms of size, sensitivity, figure of merit, and quality factor. The recommended sensor exhibits exceptional performance, making it an ideal choice for various

**Table 4**

Comparison of the sensor parameters (Substrate, Q-factor, Sensitivity and size) among different metamaterial-based liquid sensors.

Ref	Size( $\text{mm}^2$ )	Substrate	Frequency Range (GHz)	Q-Factor	Sensitivity (%)	Application
[1]	22.86 9 × 10.16	FR-4	8–12	291	0.45	Identification of fuel adulteration (Petrol & Kerosene)
[16]	10 × 10	RT 5,880	8–12	23.43	0.16	Sensing of moisture
[19]	20 × 20	FR-4	4–5	N/A	N/A	Detection of transformer oil condition
[33]	30 × 20	RT 5880	20–30	N/A	0.178	Ethanol Concentration in Liquid
[34]	50 × 40	Isolai-Tera MT40	2–6	N/A	0.39	liquid characterization
[35]	15 × 15	RO3020	2–4	N/A	0.56	Liquid dielectric Properties
[37]	58.17 × 24.50	polycarbonate	3–5	240	0.22	dielectric Properties of ethanol-methanol mixtures
[23]	35 × 35	FR-4	8–12	N/A	N/A	Identification of fuel adulteration (Diesel)
[24]	35 × 35	FR-4	8–12	N/A	N/A	detecting fluidics
[25]	23 × 23	FR-4	3.6–5.6	N/A	N/A	Vegetable Oil adulteration
Work	5 × 5	FR-4	8–12	451.58	0.57	Identification of Cooking oil and Fuel adulteration

industries, including Fuel and oil testing. Future research will focus on developing a data processing methodology and designing a versatile sensor capable of handling various applications.

## Funding

This research work was funded by the Ministry of Higher Education (MOHE) through Fundamental Research Grants Scheme (FRGS) under the Grant No FRGS/1/2021/TK0/MMU/01/1.

## CRediT authorship contribution statement

**Muhammad Amir Khalil:** Conceptualization, Investigation, Methodology, Writing – original draft. **Wong Hin Yong:** Funding acquisition, Software, Supervision, Project administration. **Ahasanul Hoque:** Supervision, Formal analysis, Validation, Writing – original draft. **Md. Shabiul Islam:** Investigation, Validation, Writing – review & editing. **Lo Yew Chiong:** Investigation, Data curation. **Cham Chin leei:** Writing – review & editing. **Saleh Albadran:** . **Mohamed S. Soliman:** Investigation, Validation. **Mohammad Tariqul Islam:** Resources, Project administration, Data curation, Visualization.

## Declaration of Competing Interest

The authors declare that they have no known competing financial interests or personal relationships that could have appeared to influence the work reported in this paper.

## References

- [1] Y.I. Abdulkarim, S. Dalgaç, F.O. Alkurt, F.F. Muhammadsharif, H.N. Awl, S. R. Saeed, O. Altintaş, C. Li, M. Bakır, M. Karaaslan, M. Ameen, R.K. Chaudhary, H. Luo, Utilization of a triple hexagonal split ring resonator (SRR) based metamaterial sensor for the improved detection of fuel adulteration, *J. Mater. Sci. Mater. Electron.* 32 (19) (2021) 24258–24272.
- [2] M. Chowdhury, A. Gholizadeh, M. Agah, Rapid detection of fuel adulteration using microfabricated gas chromatography, *Fuel* 286 (2021), 119387, <https://doi.org/10.1016/j.fuel.2020.119387>.
- [3] A. Datta, A. Saha, Investigation of an ultra-sensitive fiber-optic fuel adulteration sensor by propagating a higher-order Bessel-Gauss beam, *Optik (Stuttgart)* 243 (2021), 167408, <https://doi.org/10.1016/j.ijleo.2021.167408>.
- [4] M.N. Hossain, J. Tanvir, M.N. Aktar, K. Ahmed, Design of a fuel adulteration detector sensor based on surface plasmon resonance, *Opt Quant Electron* 55 (1) (2023).
- [5] L.M. de Aguiar, D. Galvan, E. Bona, L.A. Colnago, M.H.M. Killner, Data fusion of middle-resolution NMR spectroscopy and low-field relaxometry using the Common Dimensions Analysis (ComDim) to monitor diesel fuel adulteration, *Talanta* 236 (2022), 122838, <https://doi.org/10.1016/j.talanta.2021.122838>.
- [6] A.H.M.I. Ferdous, M.S. Anower, A. Musha, M.A. Habib, M.A. Shobug, A heptagonal PCF-based oil sensor to detect fuel adulteration using terahertz spectrum, *Sens Biosensing Res* 36 (2022), 100485, <https://doi.org/10.1016/j.sbsr.2022.100485>.
- [7] J. Bell, R. Gotor, K. Rurack, Fluorescent paper strips for the detection of diesel adulteration with smartphone read-out, *J. Vis. Exp.* 141 (2018) 2018, <https://doi.org/10.3791/58019>.
- [8] M.K.K. Figueiredo, R.P.B. Costa-Felix, L.E. Maggi, A.V. Alvarenga, G.A. Romeiro, Biofuel ethanol adulteration detection using an ultrasonic measurement method, *Fuel* 91 (1) (2012) 209–212, <https://doi.org/10.1016/j.fuel.2011.08.003>.
- [9] M.A. Khalil, W.H. Yong, M.T. Islam, A. Hoque, M.S. Islam, C.C. leei, M.S. Soliman, Double-negative metamaterial square enclosed Q.S.S.R For microwave sensing application in S-band with high sensitivity and Q-factor, *Sci Rep* 13 (1) (2023).
- [10] D.R. Smith, How to Build a Superlens, *Science* 308 (5721) (2005) 502–503.
- [11] M. Rahimi, F.B. Zarrabi, R. Ahmadian, Z. Mansouri, A. Keshtkar, Miniaturization of antenna for wireless application with difference metamaterial structures, *PIER* 145 (2014) 19–29.
- [12] K. Roy, C. Barde, P. Ranjan, R. Sinha, D. Das, A wide angle polarization insensitive multi-band metamaterial absorber for L, C, S and X band applications, *Multimed Tools Appl* 82 (6) (2023) 9399–9411.
- [13] T.A. Elwi, Metamaterial based a printed monopole antenna for sensing applications, *Int. J. RF Microwave Comput. Aided Eng.* 28 (7) (2018), <https://doi.org/10.1002/mmce.21470>.
- [14] A. Hoque and M. T. Islam, ‘Numerical Analysis of Single Negative Broadband Metamaterial Absorber Based on Tri Thin Layer Material in Visible Spectrum for Solar Cell Energy Harvesting’, doi: 10.1007/s11468-020-01132-8/Published.
- [15] M.T. Islam, A. Hoque, A.F. Almutairi, N. Amin, Left-Handed metamaterial-inspired unit cell for S-Band glucose sensing application, *Sensors* 19 (1) (2019) 169.
- [16] A. Hoque, M.T. Islam, A.F. Almutairi, M.E.H. Chowdhury, M. Samsuzzaman, SNG and DNG meta-absorber with fractional absorption band for sensing application, *Sci Rep* 10 (1) (2020), <https://doi.org/10.1038/s41598-020-69792-4>.
- [17] S. Sakib, A. Hoque, S.K.B.A. Rahim, M. Singh, N.M. Sahar, M.S. Islam, M. S. Soliman, M.T. Islam, A central spiral split rectangular-shaped metamaterial absorber surrounded by polarization-insensitive ring resonator for S-Band applications, *Materials* 16 (3) (2023) 1172.
- [18] E.L. Chuma, Y. Iano, G. Fontgalland, L.L. Bravo Roger, Microwave sensor for liquid dielectric characterization based on metamaterial complementary split ring resonator, *IEEE Sensors J.* 18 (24) (2018) 9978–9983.
- [19] O. Altintaş, M. Aksoy, E. Ünal, M. Karaaslan, Chemical liquid and transformer oil condition sensor based on metamaterial-inspired labyrinth resonator, *J Electrochem Soc* 166 (6) (2019) B482–B488, <https://doi.org/10.1149/2.1101906jes>.
- [20] N. Ullah, M. Shabirul Islam, A. Hoque, W.H. Yong, M.S. Soliman, M.T. Islam, A compact-sized four-band metamaterial-based perfect absorber for electromagnetic energy harvesting applications, *Opt Laser Technol* 168 (2024), <https://doi.org/10.1016/j.optlastec.2023.109836>.
- [21] A. Tamer, F. Karadag, E. Ünal, Y.I. Abdulkarim, L. Deng, O. Altintas, M. Bakır, M. Karaaslan, Metamaterial based sensor integrating transmission line for detection of branded and unbranded diesel fuel, *Chem Phys Lett* 742 (2020), 137169, <https://doi.org/10.1016/j.cplett.2020.137169>.
- [22] E. L. Chuma and Y. Iano, ‘Novelty Sensor using Integrated Fluorescence and Dielectric Spectroscopy to Improve Food Quality Identification’, in *Proceedings of IEEE Sensors*, Institute of Electrical and Electronics Engineers Inc., 2022. doi: 10.1109/SENSORS52175.2022.9966998.
- [23] M. Bakır, M. Karaaslan, F. Karadag, S. Dalgaç, E. Ünal, and O. Akgöl, ‘Metamaterial Sensor for Transformer Oil, and Microfluidics’.
- [24] Y. Abdulkarim, L. Deng, M. Karaaslan, S. Dalgaç, R. Mahmud, F. Ozkan Alkurt, F. Muhammedsharif, H. Awl, S. Huang, H. Luo, The detection of chemical materials with a metamaterial-based sensor incorporating oval wing resonators, *Electronics* 9 (5) (2020) 825.
- [25] O. Sopian, H.T. Yudistira, F. Qalbina, R.A. Prahma, A.G. Saputro, A. Faisal, Design of a single split-ring resonator-based microwave metamaterial for detection of the composition of vegetable oil and gasoline mixtures, *J. Mater. Sci. Mater. Electron.* 33 (10) (Apr. 2022) 8151–8158, <https://doi.org/10.1007/s10854-022-07964-w>.
- [26] M. Ali Tümkaya, M. Karaaslan, C. Sabah, Metamaterial-based high efficiency portable sensor application for determining branded and unbranded fuel oil, *Bull. Mater. Sci.* 41 (4) (2018) Aug, <https://doi.org/10.1007/s12034-018-1605-3>.
- [27] O. Altintas, M. Aksoy, O. Akgöl, E. Ünal, M. Karaaslan, C. Sabah, Fluid, Strain and rotation sensing applications by using metamaterial based sensor, *J Electrochem Soc* 164 (12) (2017) B567–B573, <https://doi.org/10.1149/2.1971712jes>.
- [28] O. Altintaş, M. Aksoy, E. Ünal, and M. Karaaslan, ‘Metamaterial inspired sensor for detection of engine lubricant oil condition’, in *AIP Conference Proceedings*, American Institute of Physics Inc., Nov. 2019. doi: 10.1063/1.5135408.
- [29] M. Bakır, Electromagnetic-based microfluidic sensor applications, *J Electrochem Soc* 164 (9) (2017) B488–B494, <https://doi.org/10.1149/2.0171712jes>.
- [30] O. Akgöl, E. Ünal, M. Bağmacı, M. Karaaslan, U.K. Sevim, M. ÖzTÜRK, A. Bhadouria, A nondestructive method for determining fiber content and fiber ratio in concretes using a metamaterial sensor based on a V-shaped resonator, *J Electron Mater* 48 (4) (2019) 2469–2481.
- [31] H. Zhou, D. Hu, C. Yang, C. Chen, J. Ji, M. Chen, Y.u. Chen, Y.a. Yang, X. Mu, Multi-Band sensing for dielectric property of chemicals using metamaterial integrated microfluidic sensor, *Sci Rep* 8 (1) (Dec. 2018), <https://doi.org/10.1038/s41598-018-32827-y>.
- [32] S. Tabassum, S.K. Nayemuzzaman, M. Kala, A. Kumar Mishra, S.K. Mishra, Metasurfaces for sensing applications: gas, bio and chemical, *Sensors* 22 (18) (2022) 6896.
- [33] S.A. Qureshi, Z.Z. Abidin, H.A. Majid, A.Y.I. Ashyap, C.H. See, Detection of ethanol concentration in liquid using a double-layered resonator operating at 5G-mm-wave frequencies, *J Electron Mater* 51 (12) (Dec. 2022) 7028–7036, <https://doi.org/10.1007/s11664-022-09932-w>.
- [34] K. Alp, F. Bagci, B. Akaoglu, A metamaterial-based dielectric sensor for characterization of ethanol/1-pentanol binary liquid mixtures at dual bands, *Appl Phys A Mater Sci Process* 129 (8) (Aug. 2023), <https://doi.org/10.1007/s00339-023-06828-2>.
- [35] S. Kayal, T. Shaw, D. Mitra, Design of metamaterial-based compact and highly sensitive microwave liquid sensor, *Appl Phys A Mater Sci Process* 126 (1) (Jan. 2020), <https://doi.org/10.1007/s00339-019-3186-4>.
- [36] V. Rawat, V. Nadkarni, S.N. Kale, Highly sensitive electrical metamaterial sensor for fuel adulteration detection, *Def Sci J* 66 (4) (Jul. 2016) 421–424, <https://doi.org/10.14429/dsj.66.10217>.
- [37] F. Bagci, M.S. Gulsu, B. Akaoglu, Dual-band measurement of complex permittivity in a microwave waveguide with a flexible, thin and sensitive metamaterial-based sensor, *Sens Actuators A Phys* 338 (2022), 113480, <https://doi.org/10.1016/j.sna.2022.113480>.
- [38] O. Altintaş, M. Aksoy, E. Ünal, Design of a metamaterial inspired omega shaped resonator based sensor for industrial implementations, *Physica E Low Dimens Syst Nanostruct* 116 (2020), 113734, <https://doi.org/10.1016/j.physe.2019.113734>.
- [39] N. Ullah, M.S. Islam, A. Hoque, W.H. Yong, M.S. Soliman, S. Albadran, M.T. Islam, A compact complementary split ring resonator (CSRR) based perfect metamaterial absorber for energy harvesting applications, *Engineering Science and Technology, an International Journal* 45 (2023), 101473, <https://doi.org/10.1016/j.jestch.2023.101473>.

- [40] N. Ullah, M.S. Islam, A. Hoque, W.H. Yong, A.M. Alrashdi, M.S. Soliman, M.T. Islam, An efficient, compact, wide-angle, wide-band, and polarization-insensitive metamaterial electromagnetic energy harvester, *Alex. Eng. J.* 82 (2023) 377–388.
- [41] M.d. Rashedul Islam, M. Tariqul Islam, A. Hoque, A.S. Alshamari, A. Alzamil, H. Alsaif, M.d. Samsuzzaman, M.S. Soliman, Star enclosed circle split ring resonator-based metamaterial sensor for fuel and oil adulteration detection, *Alex. Eng. J.* 67 (2023) 547–563.
- [42] S. Sundrasegaran, S.H. Mah, Extraction Methods of Virgin Coconut Oil and Palm-pressed Mesocarp Oil and their Phytonutrients, *eFood*, vol. 1, no. 6, John Wiley and Sons Inc, Dec. 01, 2020., 10.2991/efood.k.201106.001 381 391.
- [43] M.R. Islam, M.T. Islam, A. Hoque, M.S. Soliman, B. Bais, N.M. Sahar, S.H. A. Almaliki, Tri circle split ring resonator shaped metamaterial with mathematical modeling for oil concentration sensing, *IEEE Access* 9 (2021) 161087–161102.